Activation of the cGMP Signaling Pathway Is Essential in Delaying Oocyte Aging in Diabetes Mellitus[†,‡]

Anuradha P. Goud,[§] Pravin T. Goud,[§] Michael P. Diamond,[§] Bernard Gonik,[§] and Husam M. Abu-Soud*[,§,||]

Department of Obstetrics and Gynecology, The C.S. Mott Center for Human Growth and Development, Detroit, Michigan 48201, and Department of Biochemistry and Molecular Biology, Wayne State University School of Medicine, Detroit, Michigan 48201

Received May 8, 2006; Revised Manuscript Received July 14, 2006

ABSTRACT: Uncontrolled diabetes mellitus (DM) adversely affects oocyte maturation and embryo development via mechanisms that are yet unclear. Nonetheless, DM may cause uncoupling of nitric oxide synthases (NOSs) with reduction in the bioavailability of nitric oxide (NO), which is critical to maintain oocyte viability and prevent aging. The current study investigates the role of NO-mediated signaling related to oocyte aging in diabetic and nondiabetic mice. Age-related alterations in the oocytes, including ooplasmic microtubule dynamics (OMD), cortical granule (CG) status, and zona pellucida (ZP) hardening as well as the integrity of the spindle/chromatin were studied using confocal microscopy. Oocytes obtained from diabetic mice exhibited accelerated aging compared to that from nondiabetic mice. Moreover, oocytes from diabetic animals were exquisitely sensitive to NOS and guanylate cyclase (GC) inhibitors (L-NAME, ODQ), which induced aging and relatively resistant to its delay by the cGMP derivative (8-Br-cGMP). Oocytes from nondiabetic control mice displayed similar sensitivity to L-NAME in older oocytes, although to a significantly lower extent than that of DM ($P < 0.04-0.0001$). Despite the differences in response between DM and nonDM mice, the activation of cGMP pathway is essential to maintain the integrity of oocytes and delay oocyte aging. These findings not only indicate the role of NO signaling in the prevention of oocyte aging but also suggest enhanced aging and NO insufficiency in oocytes from diabetic mice. A comprehensive model incorporating our current findings with NOS, GC, and G kinase cycles is presented.

Diabetes mellitus (DM) is a metabolic condition characterized by elevated blood glucose levels secondary to absolute impairment of insulin secretion (type I DM). Relative impairment of insulin secretion in combination with varying degrees of peripheral resistance to insulin action leads to type II DM. The impact of diabetes on reproduction is profound, as seen by diminution in fertility and increase in reproductive losses. Elevated glucose levels before conception and during pregnancy are associated with spontaneous miscarriages, congenital malformations, and abnormalities in fetal growth and development (*1*−*4*). However, the mechanisms that contribute to these outcomes are poorly understood. It has been shown that diabetes influences the process of oocyte maturation and preimplantation embryo development (*5*−*8*). Developmental abnormalities in DM therefore, could be related to oocyte dysfunction and aging that may occur more often in DM.

Oocyte aging significantly contributes to reproductive failure, infertility and chromosome aberrations in the embryo (*9*−*13*). Moreover, oocyte aging may even be accelerated in certain circumstances (*12*, *14*). Although the exact etiological mechanisms that initiate oocyte aging are currently unknown, the specific characteristics and downstream phenomena have been partially revealed. Accordingly, aging may involve a fall in the activity of the M-phase promoting factor (MPF[1]) and the mitogen activated protein kinase (MAPK), advancement of the cell-cycle to an interphase-like state characterized by increased microtubule dynamics, altered spindle structure, and premature loss of cortical granules as well as hardening of the zona pellucida (*15*−

[†] This work was supported by the National Institutes of Health grant RO1 HL066367 (to H.M.A-S.) and the Department of Obstetrics and Gynecology, Wayne State University School of Medicine, Detroit, MI.

* To whom correspondence should be addressed. Phone: (313) 577-6178. Fax: (313) 577-8554. E-mail: habusoud@med.wayne.edu.

[‡] The work has, so far, received eight national and international awards, including the prestigious Young Investigator Award at the Gordon Research Conference in Nitric Oxide and a 1st Place Award at the Annual Junior Fellow Meeting of the American College of Obstetrics and Gynecology.

[§] The C.S. Mott Center for Human Growth and Development.

[||] Wayne State University School of Medicine.

[1] Abbreviations: NO, nitric oxide (nitrogen monoxide); SNAP, S-nitroso acetyl penicillamine; OMD, ooplasmic microtubule dynamics; CG, cortical granule; DAPI, 46 diamidino-2-phenylindole; ZP, zona pellucida; MPF, M-phase promoting factor; ART, assisted reproductive technology; IVF, in vitro fertilization; ICSI, intracytoplasmic sperm injection; MAPK, mitogen-activated protein kinase; NOS, nitric oxide synthase; H_4B, tetrahydrobiopterin; L-NAME, N^{ω}-nitro-L-arginine methyl ester; 8-Br-cGMP, 8-bromoguanosine 3′:5′-cyclic monophosphate; NADPH, β-nicotinamide adenine dinucleotide phosphate; ZP, zona pellucida; ZPDT, zona pellucida dissolution time; ODQ, 1*H*[1,2,4]oxadiazolo[4,3-*a*]quinoxalin-1-one; MTOC, microtubule organizing center; PKI, protein kinase inhibitor; CaM, calmodulin.

10.1021/bi060910e CCC: $33.50 © 2006 American Chemical Society
Published on Web 08/30/2006

Table 1: Experimental Plan Following the Study Design and Oocyte Numbers in Individual Subgroups with Specific Exposure

experiment set no.	type of exposure[a]	concn (μM)	oocyte no. ($n = 830$)	group A ($n = 406$)	group B ($n = 424$)	outcomes studied
1	L-NAME	0, 1, 10, 1000	111	53	58	ZPDT, OMD, CG status
2	oxyhemoglobin	0, 5, 100	69	34	35	ZPDT, OMD, CG status
3	ODQ	0, 0.1, 10, 100, 1000	155	76	79	ZPDT, OMD, CG status
4	cGMP-dependent PKI	0, 400, 800, 1000	216	106	110	ZPDT, OMD, CG status
5	cGMP subset 1	0, 1000, 2×10^4	99	46	53	ZPDT, OMD, CG status
	cGMP subset 2	0, 1000, 2×10^4	180	91	89	spindles and chromatin

[a] Oocytes were cultured in the presence of specified agents at the concentrations indicated.

25). Furthermore, fertilization of aged oocytes could result in abnormal fertilization, parthenogenetic activation, chromosome mis-segregation, or eventual fragmentation (*11*, *12*, *17*, *26*).

Hyperglycemia in diabetes causes a host of biochemical changes, such as increased activity of the polyol pathway, advanced glycation end-product (AGE) formation, and activation of the protein kinase C (PKC) pathway (*27*, *28*). Nonetheless, the common factor between DM and oocyte aging is the role of free radicals. The induction of free radicals in diabetes is mediated by multiple mechanisms. Reduction of endogenous antioxidant defenses due to the suppression of the pentose phosphate pathway (PRPP, phosphoribosylpyrophosphate) leads to decreased NADPH production and enhanced activity of the mitochondrial respiratory pathway, which drives the formation of the superoxide anion ($O_2^{\bullet -}$) (*29*−*31*). Both of these effects could lead to a decrease in the bioavailability of nitric oxide.

Nitric oxide (NO) is a ubiquitous free radical in the oocyte microenvironment that plays a positive role through oogenesis, fertilization, and embryo development (*32*−*33*). In animals, NO is generated by a family of enzymes named NO synthases (NOSs) which convert L-arginine to NO and citrulline (*34*−*38*). NO activates soluble guanylyl cyclase (GC) with a resultant increase in cyclic GMP (cGMP), which induces smooth muscle relaxation, affecting blood flow through vessels (*39*). However, whether NO action in the oocytes involves the same pathway remains unclear, although regulation of intracellular Ca^{2+} may be involved (*40*).

We recently discovered that NO could delay the onset of age-specific changes in oocytes at optimal concentration (*41*). Despite this knowledge, the mechanism of NO action remains speculative, especially with regard to its newly revealed anti-aging role (*40*). The current study was designed to elucidate the potential link between GC activation and aging in oocytes, compare oocyte aging in diabetic and nondiabetic mice, and study the role of NO-mediated signaling in oocytes from diabetic versus nondiabetic mice. Age-related aberrations in the oocytes, including ooplasmic microtubule dynamics (OMD), cortical granule (CG) status, and zona pellucida (ZP) hardening as well as integrity of the spindle/chromatin, were studied using fluorescent staining and confocal microscopy.

MATERIALS AND METHODS

Materials. N^{ω}-nitro-L-arginine methyl ester (L-NAME), 8-bromoguanosine 3′:5′-cyclic monophosphate (8-Br-cGMP), NO-sensitive GC inhibitor 1H (*1*, *2*, *4*) oxadiazolo [4,3-*a*] quinoxalin-1-one (ODQ), and cGMP-dependent protein kinase inhibitor (Arg-Lys-Arg-Ala-Arg-Lys-Glu) were purchased from Sigma (St. Louis, MO). Other chemicals and reagents were of the highest purity grades available and obtained from either Sigma or Aldrich (St. Louis, MO). Rhodamine-conjugated lectin, lens culinaris agglutinin, and mounting medium, Vectashield, were obtained from Vector laboratories (Burlingame, CA).

Study Design. This study was approved by Wayne State University's Animal Investigation Committee. The study consisted of the following three aims. Aim I: study of the cGMP pathway in oocytes from nondiabetic B6D2F1 mice; Aim II: comparison between oocyte aging in diabetic ALS/LtJ mice and nondiabetic age and weight matched B6D2F1 mice; and Aim III: study of NO-mediated signaling in oocytes from diabetic versus nondiabetic mice. In all aims, the oocytes were retrieved from oviductal ampullae after superovulation with PMSG and hCG (*41*). In Aim I, young and relatively old oocytes retrieved at 13.5 or 17.5 h following hCG were subjected to different treatment protocols described below, whereas their sibling oocytes were treated as controls. The treatments consisted of exposure to L-NAME, oxyhemoglobin, 8-Br-cGMP, ODQ, and the cGMP-dependent protein kinase (Table 1). All experiments included treatment of the oocytes to the microtubule enhancer, taxol, whereas those involving 8-Br-cGMP were conducted either with or without taxol treatment. In Aim II, the aging phenomena of ZPDT, OMD, and CG loss were compared in oocytes retrieved at 13.5, 16, and 18 h post-hCG from diabetic ALS/LtJ versus nondiabetic B6D2F1 mice. Aim III, oocytes retrieved from diabetic ALS/LtJ mice and B6D2F1 mice were exposed to L-NAME, SNAP, ODQ, and cGMP at several optimal concentrations. The aforementioned age-related phenomena were then compared between the two groups using appropriate statistical tests.

Superovulation and Oocyte Retrieval. Eight to ten week-old B6D2F1 and ALS/LtJ mice (Type I diabetes model) were obtained from Jackson Laboratories (Bar Harbor, ME), and were adjusted to the 14 h light−10 h dark cycle for at least

one week prior to superovulation with 7.5 IU each of pregnant mare's serum gonadotropin (PMSG) and hCG (Sigma, St. Louis, MO), administered IP 48−52 h apart. Mice were sacrificed at 13.5 to 18 h after hCG injection according to appropriate experiment sets. Cumuli retrieved from the oviductal ampullae were treated with 0.1% hyaluronidase (w/v) in M2 medium (Sigma) for 2−3 min at 37 °C. Oocytes were subsequently denuded to remove all cumulus-corona cells with a narrow bore pulled glass Pasteur pipet, thoroughly rinsed in M2 medium, inspected to rule out abnormal morphology, and kept ready in M16 medium (Sigma) pre-equilibrated with 5% CO_2 in air at 37 °C in a common pool before randomly assigning into test and control groups according to the experiment sets.

Taxol Treatment, ZP dissolution, and Tubulin and Cortical Granule Staining. Taxol 1 mM stock solution was prepared in DMSO and stored at −20 °C. Just prior to experiments, it was diluted with M2 medium containing 10% fetal bovine serum (FBS, Life Technologies) to a working concentration of 10 μM. Taxol treatment and tubulin staining was performed by the technique previously used by Goud et al. (*19*). This process was followed by zona pellucida dissolution time determination, fluorescence immunocytochemistry for α-tubulin, and cortical granule staining with rhodamine-conjugated lens culinaris agglutinin (*40*, *41*). The oocytes were thoroughly rinsed once again with the PBS TX 0.3% BSA solution prior to mounting in Vectashield with DAPI (Vector Laboratories), which contained 4′,6 diamidino-2-phenylindole (DAPI), a fluorescent chromatin stain. The oocytes were stored in glass chambers in the mounting medium at 4 °C until processing with confocal microscopy, image processing, and 3-D reconstructions (LSM 310; Carl Zeiss Inc., Thornwood, NY).

Confocal Microscopy, Assessment of Microtubules, and Cortical Granules. The cortical granules were stained fluorescent red, which was distinct from the fluorescent green staining of the microtubules (MT) and fluorescent blue staining of chromosomes. Individual treated and control oocytes from diabetic and nondiabetic mice were closely examined for spindle/ooplasmic microtubules and cortical granule status. The ooplasmic MT dynamics in response to taxol were evaluated and graded into the following three categories of microtubule dynamics, namely, minimal or negligible, moderate, and markedly increased, using the criteria described before (*41*, *42*). Similarly, the cortical granule status in each oocyte was categorized as intact CG, minor CG loss, and major CG loss (*41*, *42*). The categorization of oocytes on the basis of MT and CG status was performed by an independent observer blinded to treatment group assignment, who used comprehensive evaluation of the individual optical sections and the 3-D reconstructed images.

Aim I: Study of the cGMP Pathway in Oocytes from the Nondiabetic B6D2F1 Mice Experiment

Set 1: Exposure to L-NAME. The NOS inhibitor, L-NAME was prepared as stocks of 1 mM dissolved in distilled water and stored at −20 °C. Young (group A, $n = 53$) and old oocytes (group B, $n = 58$) retrieved as described above were exposed to L-NAME in M16 medium (0, 1, 10, and 1000 μM, 3 h, 37 °C, 5% CO_2), rinsed in M2 medium, and treated with 5 μM taxol (Paclitaxel, Sigma) per our previously published protocol (*19*, *41*, *42*). *Oocytes were then rinsed again in M2 medium and subjected to acidified Tyrode's solution, to assess the ZPDT (41). Control sibling oocytes were allowed to age in culture in M16 without L-NAME. Oocytes from either group were then fixed in freshly prepared 4% paraformaldehyde at 37 °C following taxol treatment.*

Experiment Set 2: Exposure to the NO Scavenger Oxyhemoglobin. Hemoglobin (10 mg) was dissolved in 0.1 M phosphate buffer at 37 °C. Then, 1 mg of sodium dithionite was added to the solution and passed through a PD-10 Sephadex G-25 column (Amersham Biosciences). Concentration of the eluent was measured, and dilutions were made accordingly to adjust the final concentrations to 50 μM and 100 μM.

Experiment Set 3: Exposure to Guanylyl Cyclase Inhibitor (ODQ). The NO-sensitive soluble guanylyl cyclase inhibitor, ODQ, was prepared as a 10 mM stock solution in DMSO and stored at −20 °C. Young and relatively old oocytes were exposed to ODQ (0.1, 1, 100, and 1000 μM and controls at 37 °C, and 5% CO_2, for 3 h, $n = 155$). The ODQ desired concentrations were selected on the basis of previous related studies (*43*). Subsequently, test and control oocytes were rinsed and subjected to acidified Tyrode's treatment for ZP removal and fixation in 4% paraformaldehyde at 37 °C following taxol treatment.

Experiment Set 4: Exposure to cGMP-Dependent Protein Kinase Inhibitor. The young and old oocytes were exposed to increased concentrations of the inhibitor (e.g., 400, 800, and 1000 μM (*44*)). It was prepared as stocks of 10 mM dissolved in water and stored in the −20 °C. The test and control were incubated for 3 h, rinsed and subjected to acidified Tyrode's treatment for ZP removal and fixation in 4% paraformaldehyde at 37 °C following taxol treatment.

Experiment Set 5: Exposure to 8-Bromoguanosine 3′:5′-Cyclic Monophosphate. The cGMP derivative 8-bromoguanosine 3′: 5′-cyclic monophosphate (8-Br-cGMP) was prepared as stocks of 1 M in DMSO and stored at −20 °C. The young and old oocytes were exposed to either 1 or 20 mM 8-Br-cGMP in M16 medium (37 °C, 5% CO_2, for 3 h). Exposure to 8-Br-cGMP was done in two subsets of experiments. In the first subset, the test and control oocytes were rinsed and subjected to taxol treatment and acidified Tyrode's treatment for ZP removal (*41*), followed by fixation in 4% PFA at 37 °C. In a second subset of experiments, young and relatively old oocytes exposed to 8-Br-cGMP and their sibling untreated control oocytes were fixed in 4% PFA without taxol treatment and processed for tubulin and chromatin staining. Oocytes from subset 1 were subjected to the study of ZPDT, OMD, and CG status, whereas in subset 2, the oocytes were studied for spindle and chromatin morphology (*19*, *41*).

Aim II: Comparison Between Oocyte Aging in Diabetic ALS/LtJ and Nondiabetic Mice

Oocytes were retrieved from superovulated ALS/LtJ diabetic and B6D2F1 nondiabetic control mice at 13.5, 16, and 18 h after hCG treatment (groups A, B, and C,

respectively; $n = 83$). Oocyte aging phenomena, namely, ZPDT, OMD, and CG status, were judged using above-mentioned methods. Comparisons among the groups, and between ALS/LtJ diabetic and B6D2F1 nondiabetic mice were done using the appropriate statistical tests given below.

Aim III: Study of NO-Mediated Signaling in Oocytes from ALS/LtJ Diabetic versus B6D2F1 Nondiabetic Mice

Oocytes were retrieved at 16 h after hCG from superovulated ALS/LtJ diabetic and B6D2F1 nondiabetic mice and were exposed to the following treatments ($n = 161$): (1) SNAP (100 μM, 0.11 μM/min NO), (2) L-NAME, (3) ODQ, and (4) 8-Br-cGMP using methods described in Aim I. Oocyte aging phenomena of ZPDT, OMD, and CG loss were then evaluated and compared between oocytes from diabetic ALS/LtJ and nondiabetic B6D2F1 mice using the appropriate statistical tests given below.

Statistical Tests. Statistical analysis was performed using SPSS version 11.0 (SPSS Inc., Chicago, IL). The frequency data in each test and control subgroup were analyzed using chi square tests. Frequencies of microtubule dynamics and CG status as well as spindles in individual subgroups with various exposures within groups young and relatively old were compared to their respective sibling control oocyte subgroups using Fisher's exact test. The data on zona pellucida dissolution timings were compared between test and control subgroups using the student's unpaired *t*-test. Differences in ZP dissolution timings among subgroups exposed to individual concentrations were analyzed using one-way ANOVA and the Student−Newman−Keuls post-hoc test. Where appropriate, raw data underwent log transformation prior to statistical analysis. Data were represented as mean ± SD. Significance was defined as $P < 0.05$.

RESULTS

Aim I: Study of the cGMP Pathway in Oocytes from Nondiabetic B6D2F1 Mice. A total of 830 oocytes retrieved at 13.5 (young, $n = 406$) and 17.5 h (relatively old, $n = 424$) were utilized in five experiment sets, of which the fifth experiment set (8-bromo-cGMP) comprised two subsets. The experiments included oocytes exposed to an individual agent ($n = 559$) as well as unexposed control sibling oocytes ($n = 271$). The numbers of oocytes in each experiment set and concentrations of individual agents as well as the outcomes studied are presented in Table 1.

Exposure of Young and Old Oocytes to L-NAME. Experiment set 1 included young (group A, $n = 53$) and relatively old oocytes (group B, $n = 58$). Of these, 56 oocytes exposed to L-NAME were compared to corresponding sibling unexposed control oocytes ($n = 35$). In young oocytes exposed to L-NAME, the ZPDT did not show any difference between the exposed versus unexposed control oocytes at 1 μM concentration. Nonetheless, a small but significant increase in ZPDT was noticed at 10 μM ($P = 0.039$), which became highly significant at 1 mM concentration ($P < 0.0001$, Figure 1A). In contrast, relatively older oocytes from group B showed a highly significant increase in ZPDT at all concentrations studied ($P < 0.0001$), indicating their higher sensitivity to L-NAME compared to that of group A (Figure 1B). Interestingly, the ZPDT of young oocytes exposed to 1 mM L-NAME were comparable to unexposed control oocytes from group B (Figures 1A and B).

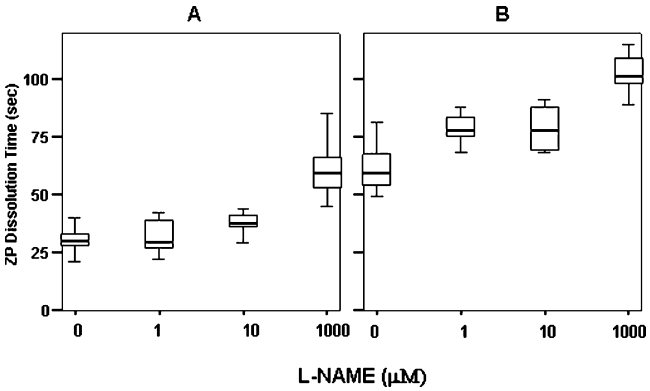

FIGURE 1: ZPDT of L-NAME treated and untreated young and relatively old oocytes. A box and whiskers plot representing the ZPDT of young (group A) and relatively old oocytes (group B) exposed to L-NAME (1, 10, and 1000 μM) and untreated controls. A significant increase in ZPDT was noted in group A (young oocytes) exposed to 10 and 1000 μM L-NAME ($P = 0.039$ and <0.0001, respectively) and in group B (relatively old oocytes) exposed to 1, 10, and 1000 μM L-NAME compared to that of respective controls ($P < 0.0001$).

An analysis of the microtubule dynamics in oocytes exposed to L-NAME versus controls showed no differences in those with minimal or moderate microtubule dynamics. Nonetheless, there was a significant increase in oocytes with markedly increased microtubule dynamics in group A, which were exposed to L-NAME at 1 mM concentration, and at all concentrations studied in group B compared to controls (Figure 2).

Oocytes from group A that were exposed to L-NAME showed no difference in CG status at 1 and 10 μM. However, significantly fewer oocytes from group A exposed to L-NAME had intact CG ($P = 0.003$). On the contrary, in group B, among the oocytes exposed to L-NAME at 10 μM and 1 mM, significantly fewer oocytes had intact CG. Likewise, old oocytes also showed a significant increase in the incidence of oocytes with major CG loss after exposure to all of the above concentrations of L-NAME. However, among young oocytes, major CG loss occurred among L-NAME-exposed oocytes at 1 mM concentration (Figure 2).

Exposure to Oxyhemoglobin. In group A, young oocytes exposed to oxyhemoglobin at 5 μM showed no significant differences in ZPDT, OMD, or the CG status. However, a significant increase was noted in ZPDT among oocytes exposed to 100 μM oxyhemoglobin ($P < 0.001$). Also in group A, a small increase in oocytes with markedly increased microtubule dynamics was noted at 100 μM (0 vs 27.3%), which, however, was not statistically significant.

In group B, oocytes exposed to both 5 and 100 μM showed an increase in ZPDT ($P < 0.0001$) and OMD ($P = 0.027$ and 0.001 at 5 and 100 μM, respectively; Figure 3). Similarly, a significant decrease in the numbers of oocytes with intact CG (5 μM, $P = 0.012$; 100 μM, $P = 0.003$) and a significant increase in oocytes with major CG loss were observed among oocytes in group B exposed to 5 μM ($P = 0.027$) as well as 100 μM oxyhemoglobin ($P = 0.001$).

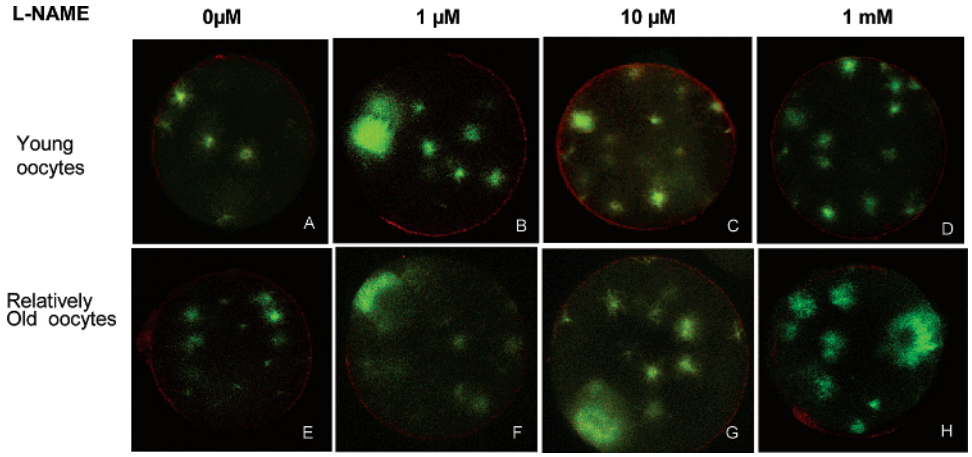

FIGURE 2: Fluorescence photomicrographs of oocytes stained for α-tubulin (FITC, green) and CG (rhodamine, red) after exposure to different concentrations of L-NAME followed by taxol treatment. An increase in ooplasmic microtubule dynamics is notable in the form of increased free microtubules and asters in B−D and F−H compared to that in young oocytes (A) in the presence of increasing L-NAME concentrations (1, 10, 1000 μM). Controls of relatively old oocytes (E) show moderately increased microtubules. Also notable are intact cortical granules (CG) along the oocyte periphery in A, B, C, and E. Minimal CG loss is noted in F and G, and a major CG loss is observed in D and H. Original magnification: 400−600×; average oocyte diameter is 70−80 μm.

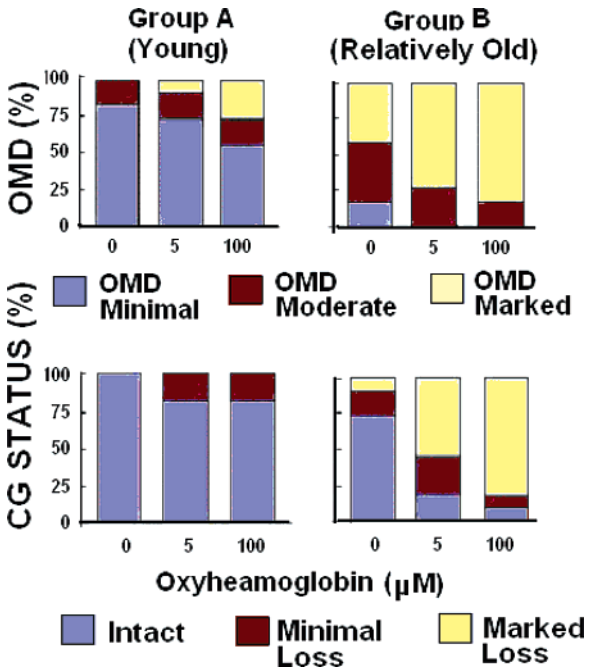

FIGURE 3: Effect of oxyhemoglobin treatment on young and relatively old oocytes. A composite of bar charts, ooplasmic microtubule dynamics, and CG status in young (group A) and relatively old oocytes (group B) after exposure to oxyhemoglobin (0, 5, and 100 μM). A significant increase in OMD (upper panel) and CG (lower panel) loss was prominently noted among the oocytes from group B.

Exposure to Guanylyl Cyclase Inhibitor (ODQ). Oocytes from groups A and B both showed significant alterations in the aging phenomena of ZPDT, OMD, and CG loss on exposure to ODQ. The ZPDT showed a progressive increase with increasing concentrations of ODQ in both groups, A and B (data not shown). However, OMD and CG loss increased at higher concentrations. An increase in OMD was noted in group A, as assessed by higher numbers of oocytes with markedly increased OMD (100 μM, $P = 0.001$; 1 mM, $P < 0.0001$) and lower numbers of oocytes with minimal OMD (100 μM, $P = 0.001$; 1 mM, $P = 0.002$). The hallmark of increased OMD was also seen in the form of increased size and numbers of microtubular asters arising from the microtubule organizing centers (MTOC, Figure 4). The young (group A) and relatively aged oocytes (group B) also showed a major CG loss at 100 μM (group A, $P = 0.005$; group B, $P = 0.021$) and 1 mM ODQ (group A, $P = 0.004$; group B, $P = 0.038$). Similarly, fewer oocytes bearing intact CG were observed among those exposed to ODQ at 100 μM (group A, $P = 0.006$; group B, $P = 0.009$) and 1 mM (group A, $P = 0.004$; group B, $P = 0.019$).

Exposure to cGMP-Dependent Protein Kinase Inhibitor. In groups A and B, significant increases in ZPDT and OMD as well as CG loss were seen among oocytes exposed to 800 μM and 1 mM cGMP PKI. Nonetheless, the increase in these parameters was smaller at 400 μM concentration, significant only for ZPDT in group B ($P < 0.01$). Oocyte treatment with the peptide brought about a significant elevation in microtubule turnover (OMD), as seen from an increase in the numbers of oocytes with markedly increased OMD (group A, 800 μM, $P = 0.048$; 1 mM, $P = 0.001$; group B, 800 μM, $P = 0.001$; 1 mM, $P < 0.0001$) and a decrease in those with minimal OMD (group A, 800 μM, $P = 0.009$; 1 mM, $P < 0.0001$; group B, 800 μM, $P = 0.031$; 1 mM, $P = 0.028$). Similar results were also noted with regard to CG status because more oocytes exposed to cGMP PKI had major CG loss in group A (800 μM, $P = 0.002$; 1 mM, $P < 0.0001$) and group B (800 μM, $P = 0.020$; 1 mM, $P = 0.007$; Figure 5).

Exposure to 8-Bromoguanosine 3′:5′-Cyclic Monophosphate. Exposure to the cGMP derivative significantly decreased the ZPDT in both group A and B. This effect was observed at both concentrations studied, namely, 1 and 20 mM, respectively ($P < 0.0001$ for all; Figure 6A and B). Among the oocytes studied for OMD, group A had significantly higher numbers of oocytes with minimal OMD and significantly lower numbers of those with moderate OMD at both 1 and 20 mM ($P = 0.005$). There was no difference in the response to 1 and 20 mM 8-Br-cGMP. However,

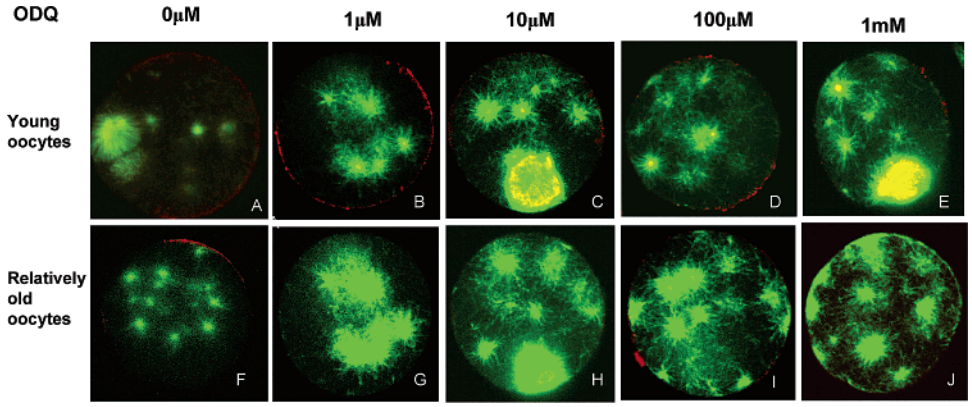

FIGURE 4: Effect of sGC inhibitor, ODQ, on young and relatively old oocytes. A composite of photomicrographs reveals optical sections from young (B−E) or relatively old (G−J) oocytes treated with different concentrations of ODQ (1, 10, 100, and 1000 μM). The oocytes were stained for α-tubulin with antibody (FITC, green), rhodamine-conjugated lens culinaris agglutinin (LCA, red) and DAPI (blue) for microtubules, CG, and chromatin, respectively. The oocytes represented in the composite show enhanced microtubule dynamics (B−E and G−J) compared to that of the control young (A) and relatively old oocytes (F). See text for further details. Original magnification = 400−600×; average oocyte diameter is 70−80 μm.

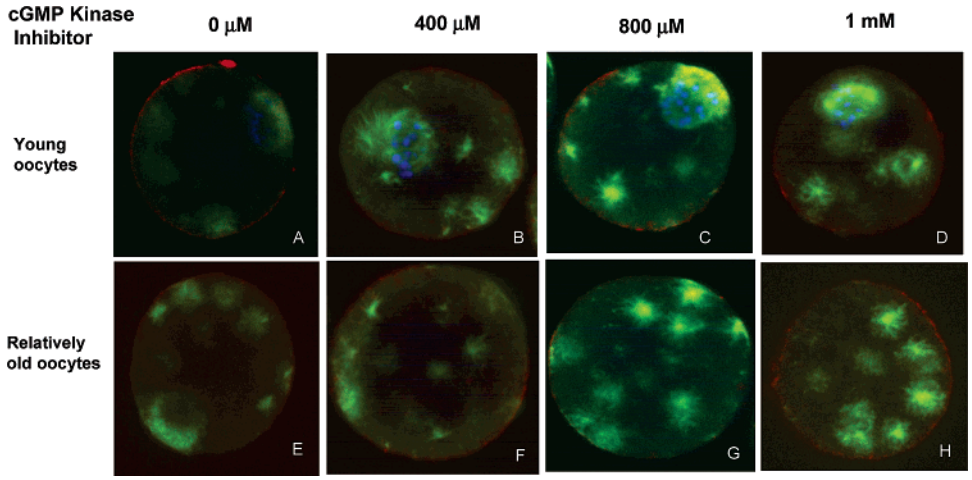

FIGURE 5: Fluorescent photomicrographs depict young and relatively old oocytes treated with different concentrations of cGMP kinase inhibitor. An increase in microtubule activity is noted in the young oocytes (B−D) and the relatively old oocytes (F−H) after exposure to increasing concentrations of cGMP kinase inhibitor (400, 800, and 1000 μM). Blue (DAPI) depicts the chromatin, red (rhodamine) the CG, and green (FITC) the microtubules. Control young and relatively old oocytes are depicted in optical images A and E, respectively. Original magnification = 400−600×; average ooxyte diameter is 70−80 μm.

oocytes from group B exposed to 8-Br-cGMP showed a significant increase in the numbers of oocytes with minimal OMD ($P < 0.0001$). A corresponding significant decrease in the numbers was also seen in the proportion of oocytes with marked OMD in group B at both concentrations studied ($P < 0.0001$; Figure 7).

Among the oocytes studied for CG status, oocytes from group A did not reveal significant differences despite exposure to 8-Br-cGMP at either 1 or 20 mM. Nonetheless, the oocytes from group B showed a significant increase in oocytes with intact CG and a corresponding significant decrease in those with major CG loss at 1 mM ($P < 0.0001$) and 20 mM of 8-Br-cGMP ($P = 0.001$; Figure 7).

In the second subset of experiments, oocytes exposed to 8-Br-cGMP showed a significant decrease in the spindle and chromatin abnormalities (6.4 and 6.7% at 1 and 20 mM, respectively, vs that of controls; $P = 0.044$). Oocytes with normal and abnormal spindle morphology after exposure to 8-Br-cGMP in old oocytes are shown in Figure 7.

Aim II: Comparison Between Oocyte Aging in Diabetic ALS/ LtJ and Nondiabetic Mice. In total, 83 oocytes from ALS/LtJ and B6D2F1 mice, retrieved at 13.5, 16, and 18 h post-hCG, were used to study and compare the aging phenomena of ZPDT, OMD, and CG loss. The response to superovulation with PMSG and hCG was lower to a certain extent in diabetic mice as seen from significantly lower numbers of oocytes retrieved per animal compared to that from nondiabetic mice at all post-hCG intervals ([36 from 5] 7.2 vs [47 from 2] 23.5 per animal, respectively; $P < 0.05$). Furthermore, oocytes from diabetic animals displayed a significant increase in the occurrence of aging phenomena.

The ZP dissolution time in oocytes from ALS/LtJ diabetic mice was similar to those from nondiabetic B6D2F1 mice in group A. However, the ZPDT increased significantly with postovulatory aging in oocytes from both diabetic and nondiabetic mice. Thus, oocytes from diabetic mice exhibited significantly increased ZPDT in groups B and C (Figure 8A, $P < 0.0001$). Moreover, the increase in ZPDT with posto-

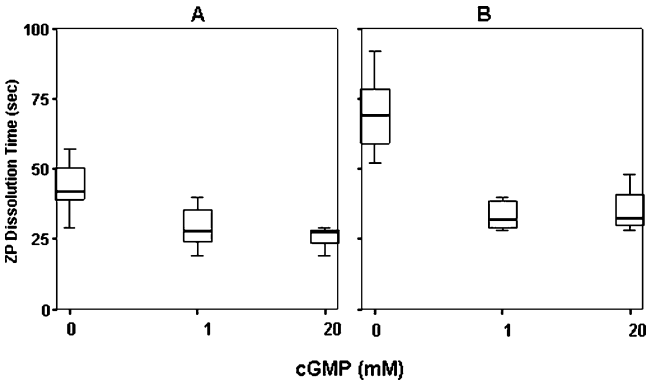

FIGURE 6: A box and whiskers plot representing the ZPDT of young (group A) and relatively old oocytes (group B) exposed to cGMP and controls. (A) In group A, a significant decrease in ZPDT was noted in young oocytes exposed to 1 and 20 mM cGMP compared to that in respective untreated controls (*$P < 0.0001$). (B) In group B, relatively old oocytes exposed to 1 and 20 mM cGMP were compared to their respective untreated controls (*$P < 0.0001$).

vulatory age was significantly higher in diabetic versus nondiabetic mice ($F = 23.7$, $df = 2, 77$; $P < 0.0001$).

The oocytes from diabetic ALS/LtJ mice and B6D2F1 mice, however, differed in OMD in groups A and B. In group A, the diabetic mice had significantly fewer oocytes with minimal OMD and significantly more oocytes with moderately increased OMD ($P = 0.001$, Figure 8B), whereas, in group B, diabetic mice had significantly fewer oocytes with minimal and moderate OMD but significantly more oocytes with markedly increased OMD ($P < 0.0001$). However, diabetic ALS/LtJ mice also displayed significantly fewer oocytes with intact CG ($P = 0.028$) and significantly more oocytes with minimal and marked CG loss, respectively ($P < 0.0001$, Figure 8C).

Aim III: Study of NO-Mediated Signaling in Oocytes from ALS/LtJ Diabetic Versus B6D2F1 Nondiabetic Mice. In this series of experiments, oocytes retrieved from ALS/LtJ diabetic mice and B6D2F1 nondiabetic mice at 16 h post-hCG, were exposed to the NO donor, SNAP, the NOS inhibitor, L-NAME, the GC inhibitor, ODQ, or the cGMP derivative, 8-Br-cGMP. Oocyte aging was assessed by determining the ZPDT, OMD, and CG status in exposed oocytes and controls.

Among oocytes that were unexposed to any of the above agents, a significant increase in ZPDT was noted in diabetic ALS/LtJ oocytes versus nondiabetic B6D2F1 mice ($P = 0.01$). Exposure to SNAP caused a significant decrease in ZPDT in oocytes from both diabetic versus control nondiabetic mice ($P = 0.01$). However, the extent of this protective effect of SNAP was similar between the diabetic and nondiabetic mice. Exposure to L-NAME increased the ZPDT in diabetic as well as nondiabetic mice. However, the increase was significantly accelerated in diabetic mice compared to that in nondiabetic mice ($P = 0.009$). The oocytes from diabetic mice were, therefore, more sensitive to L-NAME in this regard than nondiabetic mice (Figure 10).

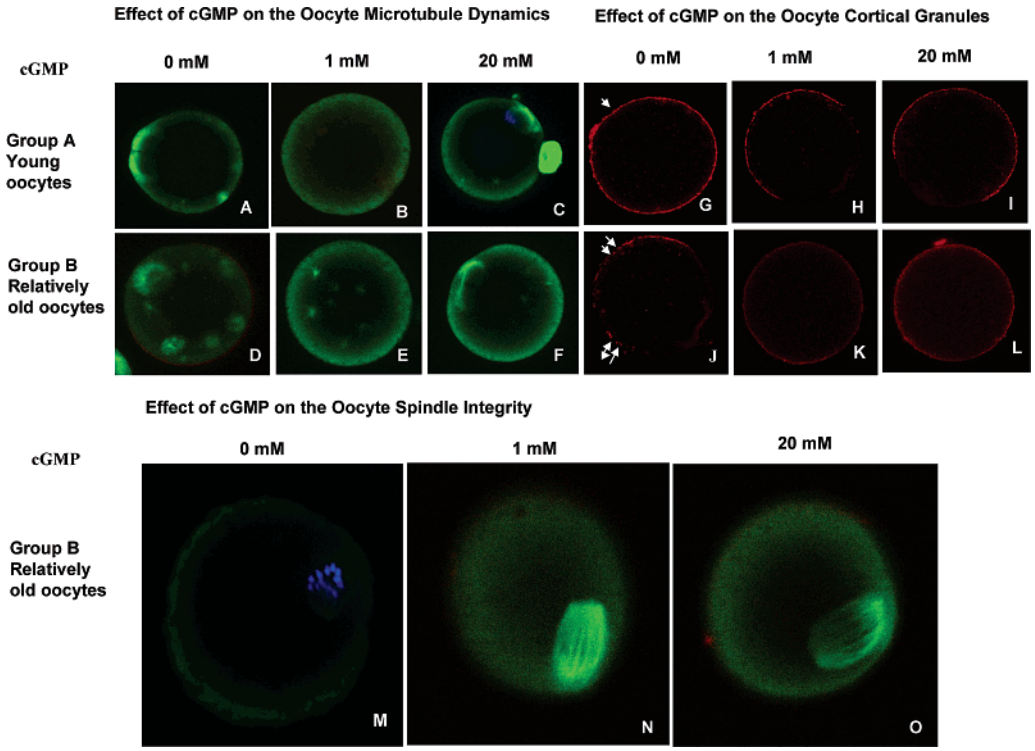

FIGURE 7: Fluorescence photomicrographs of oocytes stained for α-tubulin (FITC, green), chromatin (DAPI, blue), and cortical granules (rhodamine, red) after exposure to 8-Br-cGMP. The upper panel shows a decrease in microtubules is observed in both young and relatively old oocytes treated with 8-Br-cGMP (1 and 20 mM) despite taxol treatment. Treated young oocytes (B and C) and relatively old oocytes (E and F) display negligible MT compared with that of the young control (A) and old control (D). Similarly, control young oocyte (G) displays some CG aggregation and exocytosis (arrowhead points to exocytosis), whereas, a control relatively old oocyte (J) displays CG loss (twin arrowheads). Oocytes exposed to 8-Br-cGMP (H, I, K, and L) have an intact rim of CG along the periphery, barring the CG-free domain in the spindle zone. The CG was stained with rhodamine-conjugated lens culinaris agglutinin. The lower panel shows oocytes that were either untreated control oocytes from group B (M), or those treated with 1 mM (N) or 20 mM (O) 8-Br-cGMP. Intact spindles are visualized in N and O. However, the control relatively old oocyte (M) depicts displacement of chromosomes (arrowhead) from the metaphase plate (DAPI, blue). Original magnification = 400−600×; average oocyte diameter is 70−80 μm.

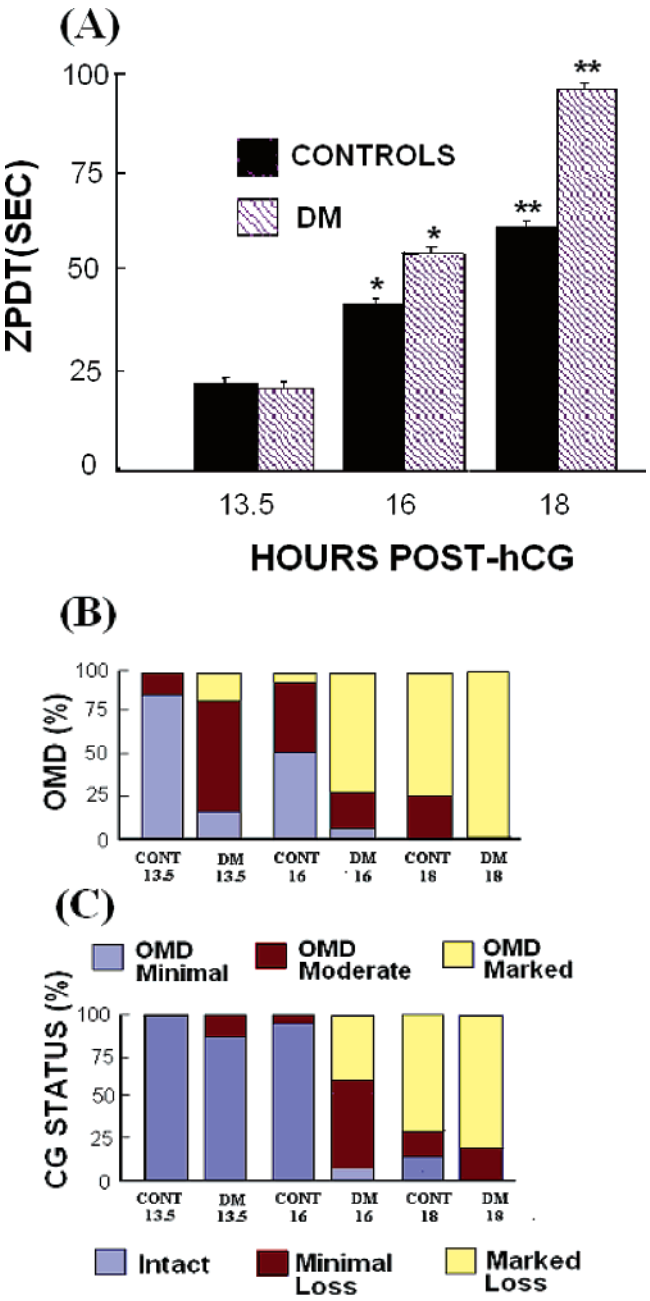

FIGURE 8: Bar charts depicting ZPDT (s) (A), OMD, and CG status. Among oocytes obtained from nondiabetic mice (B) and diabetic mice (C) 13.5, 16, and 18 h post-hCG, (A) ZPDT shows significant increase at 16 and 18 h in oocytes from diabetic mice (* , ** ($P <$ 0.0001)). Also, the percent ZPDT increase with postovulatory age was significantly higher in the oocytes from mice with diabetes mellitus (DM) versus that in nondiabetic mice (CONT) ($F = 23.7$ $df = 2, 77$; $P < 0.0001$). (B) The bar chart represents the percentage of oocytes with minimal, moderate, or marked OMD. Significantly higher numbers of oocytes displayed minimal OMD in nondiabetic vs diabetic mice at 13.5, 16, and 18 h post-hCG ($P < 0.0001$), whereas the oocytes with markedly increased OMD were significantly higher in the oocytes from DM compared to those from nondiabetic animals ($P < 0.0001$). Similarly, oocytes bearing intact CG were significantly higher and CG loss was lower in oocytes from nondiabetic mice versus diabetic mice.

An assessment of OMD and CG status revealed significantly lower numbers of oocytes with minimal OMD and intact CGs. Significantly higher numbers of oocytes with markedly increased OMD and CG loss were observed in diabetic mice compared to those in nondiabetic mice. However, the exposure of SNAP significantly decreased oocytes with moderate and markedly increased OMD and increased CG loss. L-NAME exposure led to the opposite effect with significantly increased numbers of oocytes with increased OMD and CG loss in diabetic and nondiabetic mice. Nonetheless, the effect of L-NAME was augmented in diabetic mice as seen from the significant percent change in oocytes with increased OMD and CG loss, compared to that in nondiabetic B6D2F1 mice ($t = 2.9$, $df = 1, 19$; $P = 0.009$; Figure 10).

Exposure to the GC inhibitor, ODQ, increased the aging phenomena of ZPDT and OMD as well as CG loss in oocytes from diabetic and nondiabetic mice ($P < 0.0001$). Significantly more oocytes exposed to ODQ had markedly increased OMD and CG loss compared to those of unexposed control oocytes in both diabetic and nondiabetic control oocytes (Figures 9 and 11).

Exposure to 8-Br-cGMP resulted in significantly lower ZPDT ($P < 0.0001$), significantly more oocytes with minimal OMD and intact CGs, and significantly fewer oocytes with markedly increased OMD and CG loss in both diabetic ALS/LtJ and nondiabetic B6D2F1 mice. Nevertheless, the effect of 8-Br-cGMP was seen only at $\geq$20 mM concentrations in diabetic mice, whereas the same was observed at 1, 10, and 20 mM concentrations in nondiabetic mice (Figures 9 and 11).

DISCUSSION

Metabolic derangements prevailing around conception significantly increase the risk of spontaneous miscarriages and congenital malformations in females with diabetes mellitus. Even more interesting is the concept of oocyte dysfunction in diabetic subjects because oocytes have the machinery to modulate/program the genes crucial for development (*45*). However, the pathophysiologic mechanisms in DM that lead to embryonic abnormalities are unclear. Nonetheless, free radicals have emerged as major players in diabetic pathophysiology with involvement in a plethora of reactions that could affect oocytes and embryos, just as other tissues/organs do in DM. Among these, the role of NO is particularly under scrutiny, and diminished NO may be implicated in complications related to DM (*46*−*49*). We recently demonstrated that NO delays oocyte aging and improves the integrity of the microtubular spindle apparatus (*41*). Thus, understanding the consequences of NO loss on oocyte viability and identifying the conditions in which NO regulation contributes to oocyte aging are topics of considerable interest and potential importance.

Our current results clearly demonstrate that oocytes in DM are more vulnerable to aging than those from the matched controls, as judged by the significantly increased ZPDT, OMD, and CG loss in oocytes. Similarly, supplementation with NO significantly prevented oocyte aging in both diabetic and nondiabetic animals. An increase in Ca^{2+} level is a hallmark of oocyte aging. Because NO-mediated cGMP accumulation prevents oocyte aging, a decrease in Ca^{2+} level akin to the vascular smooth muscles may also occur in oocytes. These processes can prevent calmodulin kinase activation and consequent cyclin ubiquitation. Likewise,

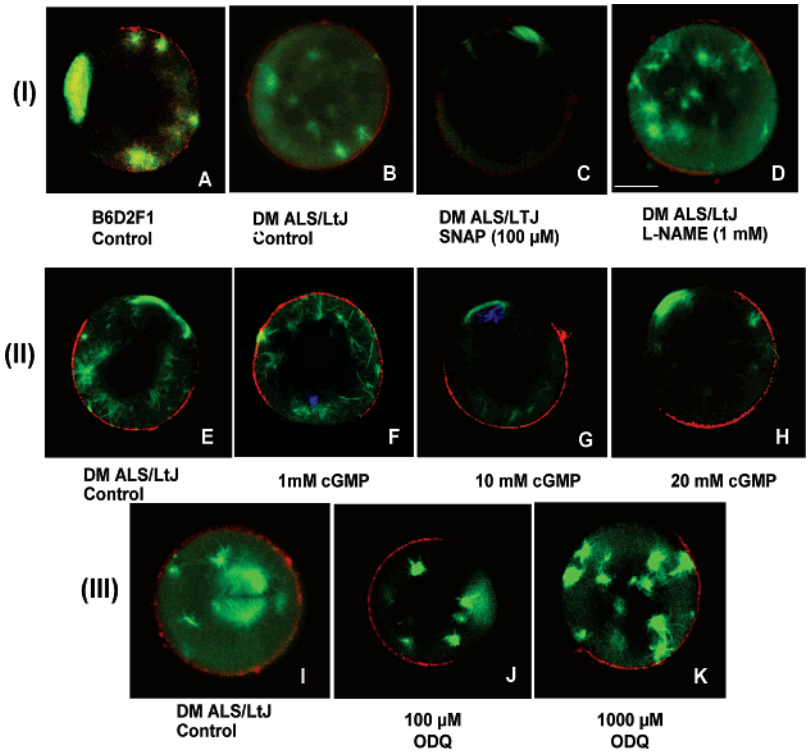

FIGURE 9: Effect of SNAP, L-NAME, cGMP, and ODQ in oocytes from diabetic mice. (I) Fluorescence photomicrographs of the oocytes stained for α-tubulin with antibody (FITC, green), rhodamine-conjugated lens culinaris agglutinin (LCA, red), and DAPI (blue). (I-A) Oocytes exposed to 10 μM taxol for 5 min prior to fixation in normal B6D2F1 mice oocytes. (I-B) Exposure to 10 μM taxol for 5 min prior to fixation of the ALS/LtJ mice oocytes. A significant enhancement of the OMD is seen in oocytes from DM mice compared to that of the healthy mice. (I-C) Exposure to 100 μM of NO donor *S-nitroso acetyl penicillamine* (SNAP, estimated NO release = 0.23 μM/min,) for 3 h. NO supplementation in oocytes retrieved at 16 h post-hCG from DM mice resulted in a significant diminution in OMD and CG exocytosis compared to those of untreated control oocytes from DM mice (I-B). (I-D) Exposure to 1mM L-NAME followed by taxol treatment. An increase in ooplasmic microtubule dynamics is notable in the form of increased free microtubules. (II) Fluorescence photomicrographs of oocytes after exposure to 8-Br-cGMP. Diabetic oocytes (E−H) are treated with 1, 10, and 20 mM 8-Br-cGMP, respectively. There is a definite decrease in the OMD of diabetic oocytes with the treatment with 8-Br-cGMP at concentrations of 10 and 20 mM. There is no effect of the 1mM 8-Br-cGMP in diabetic oocytes. Oocytes from DM mice show moderately increased microtubules in the untreated control oocytes compared to those in the 8-Br-cGMP treated oocytes. (III) Composite of photomicrographs revealing optical sections from (I-K) oocytes treated with different concentrations of ODQ (100 and 1000 μM). The oocytes represented in the composite show enhanced microtubule dynamics in the form of asters compared to that of the untreated diabetic oocytes. Original magnification = 400-600×; average oocyte diameter is 70−80 μm.

cGMP may prevent the phosphorylation of tyrosine and threonine residues in cdc-2 kinase (MPF), and both of these events prevent MPF inactivation due to aging.

A working model that incorporates our current findings with NOS, GC, and G-kinase cycles is shown in Figure 12. In this model, NOSs are homodimer enzymes that require FMN, FAD, H_4B, calmodulin (CaM), and NADPH to convert L-Arg and molecular O_2 to citrulline and NO (*34*, *35*) (Figure 12A). Both L-Arg and H_4B play a crucial role in NOS coupling, and their deficiency allows the enzyme to generate $O_2^{\bullet-}$ instead of NO (*50*−*53*). L-NAME binds within the substrate-binding site of NOS and renders electron flux through the enzyme system (*50*) (Figure 12A).

Our results indicate that the L-NAME concentrations required for the induction of the aging phenomena were 10^2−10^3-fold higher in young compared to that in relatively old nondiabetic oocytes. L-NAME also accelerated age-related changes in diabetic animals compared to that in nondiabetic controls. Because L-NAME is a NOS inhibitor, we can conclude that oocyte aging is associated with a depletion of L-Arg, H_4B, and/or NOS expression. This process, consequently, leads to a decrease in endogenous NO bioavailability. Indeed, decreased levels of NO are known to occur in different tissues in DM and are implicated in the pathogenesis of diabetes-related complications. Goto−Kakizaki rats were found to produce less NO in aortic tissues due to NOS uncoupling (*47*). Similarly, eNOS mRNA levels in diabetic db/db mouse aortic endothelial cells were reduced by 60% compared to that in control C57BL/6J mice (*48*).

Soluble guanylate cyclase is the only known receptor for NO characterized so far (*54*, *55*). It is a heterodimeric hemoprotein composed of α- and β-subunits and catalyzes the conversion of GTP to cGMP and pyrophosphate (*37*, *56*, *57*). The ferrous heme iron is ligated to the β-subunit through a histidine nitrogen, which forms a six-coordinate ferrous−nitrosyl complex (*37*, *56*, *57*). The formation of such a complex triggers a conformational change in sGC through the cleavage of the proximal histidine ligand resulting in a five-coordinate high-spin NO adduct, which subsequently becomes a free platform to catalyze the conversion of GTP to cGMP (*37*, *56*, *57*) (Figure 12B).

Inactivation of sGC in both nondiabetic and diabetic mice by ODQ, an inhibitor of sGC by heme oxidation, preventing NO-mediated stimulation resulted in enhanced tubulin polymerization with an increase in microtubule turnover

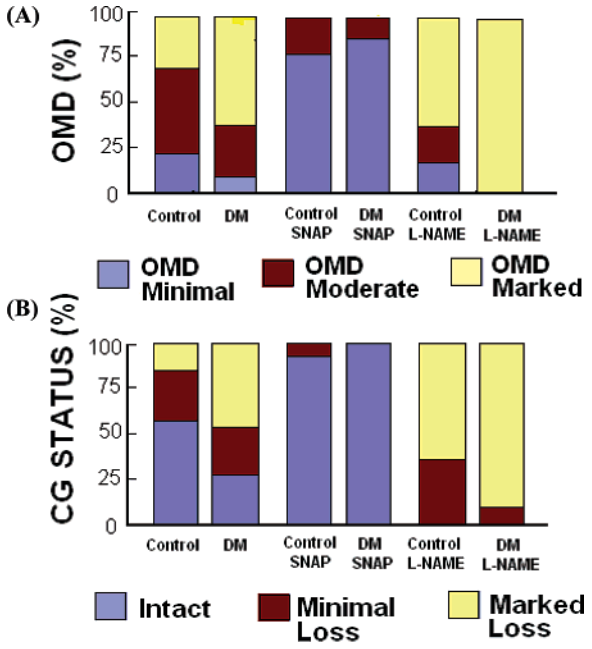

FIGURE 10: Bar charts depicting the OMD (A) and the CG status (B) among oocytes from nondiabetic mice and diabetic mice exposed to the NO donor SNAP and the NOS inhibitor L-NAME. Exposure to L-NAME resulted in a significant increase in the OMD and CG loss ($P = 0.01$). Exposure to SNAP resulted in a significant improvement in the OMD and the CG status as seen from the significantly higher numbers of oocytes bearing minimal OMD and intact CGs ($P = 0.009$).

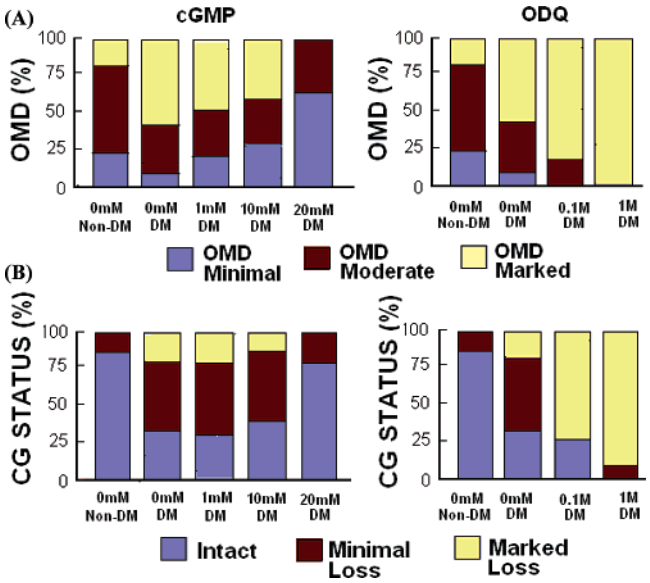

FIGURE 11: Compilation of bar charts depicting the ooplasmic microtubule dynamics and cortical granule status among oocytes exposed to the cGMP derivative 8-Br-cGMP and the NOS inhibitor, ODQ. (A) Similar to the findings in Aim II, oocytes from the diabetic ALS/LtJ mice revealed increased OMD and CG loss compared to those from the nondiabetic B6D2F1 mice ($P < 0.0001$). On exposure to 8-Br-cGMP, the oocytes from diabetic mice underwent diminution in OMD as seen from the significantly higher numbers of oocytes bearing minimal OMD compared to the unexposed diabetic mice. However, this effect was significant only at 20 mM concentration ($P < 0.0001$). (B) The CG status of the oocytes exposed to 8-Br-cGMP also revealed a significant improvement at 20 mM concentration as seen from the significantly higher numbers of oocytes with intact CG and significantly fewer oocytes with CG loss ($P < 0.0001$). (C) and (D) However, exposure to ODQ resulted in a significant deterioration in the OMD and CG status as seen from significantly higher numbers of oocytes bearing marked OMD and CG loss, and the effect was seen at both concentrations of ODQ ($P < 0.0001$).

in the ooplasm and augmented CG loss. Likewise, similar results were noted in conjunction with NO inhibition/scavenging experiments. These findings support the notion that NO mediates sGC activation, consequently preventing oocyte aging (*41*). Consistent with this hypothesis, the exposure of oocytes to 8-Br-cGMP prevented oocyte aging and improved oocyte integrity and quality (Figure 12B). However, a major difference in the oocytes from diabetic mice was that the response to cGMP occurred only at 20 mM, whereas in nondiabetic mice, the effect of 8-Br-cGMP in terms of delaying aging occurs at 1 mM. Thus, oocytes obtained from diabetic mice may have suffered a cGMP deficit due to NO deprivation despite an intact functional cGMP-dependent signaling pathway. Hence, NO treatment can protect oocytes from aging to the same extent in both nondiabetic and diabetic mice. Thus, the activation of the NO-mediated signaling pathway is essential in maintaining oocyte integrity and function. Whereas, compromise in NO-bioavailability and perturbed cGMP signaling may contribute to oocyte dysfunction in the form of enhanced oocyte aging, which is particularly accelerated in DM, this may also explain the embryo failure that occurs frequently in DM (*58*, *59*).

One of the critical downstream mechanisms mediating postovulatory oocyte aging is the increase in cytosolic Ca^{2+} that occurs because of the failure of the Ca^{2+} pumps in the endoplasmic reticulum (ER) and the cell membrane. Prevention of this step may take place via NO-mediated regulation of Ca^{2+} release (Figure 12C). Cyclic GMP-dependent reduction of intracellular free Ca^{2+} is a critical step involved in this pathway (*39*, *60*, *61*). This decrease in intracellular Ca^{2+} may be secondary to the inhibition of inositol 1,4,5-trisphosphate ($InsP_3$) induced Ca^{2+} release by activating the cGMP-PK (*62*). It could also occur because of PDE III inhibition leading to increased cAMP, which activates cAMP protein kinase (cAMP-PK, (*63*)). One other mechanism, which could explain the NO-dependent inhibition of Ca^{2+} release, is the inhibition of $InsP_3$ formation via the inhibition of phospholipase C or phospholipase C-G protein receptor coupling (*64*−*66*). Similarly, cGMP released through the action of NO on soluble guanylate cyclase also regulates Ca^{2+} release via ryanodine receptors (*67*).

Oxidative stress is considered as a potential candidate responsible for the initiation of aging. One of the major sources of oxidative stress is the formation of $O_2^{\bullet-}$. Under normal circumstances, $O_2^{\bullet-}$ is metabolized by superoxide dismutase and other mechanisms requiring NADPH as a cofactor. Under pathological conditions, where L-Arg and/or H_4B are depleted, the NOS leads to the formation of $O_2^{\bullet-}$ instead of NO (Figure 12A). Superoxide formation (possibly from NOS uncoupling or other sources) may also scavenge NO, further exacerbating the oocyte aging process. Superoxide and H_2O_2, a mediator as well as an intermediate molecule produced during the metabolism of $O_2^{\bullet-}$, induce changes in oocyte Ca^{2+} release patterns that are akin to aging (*68*).

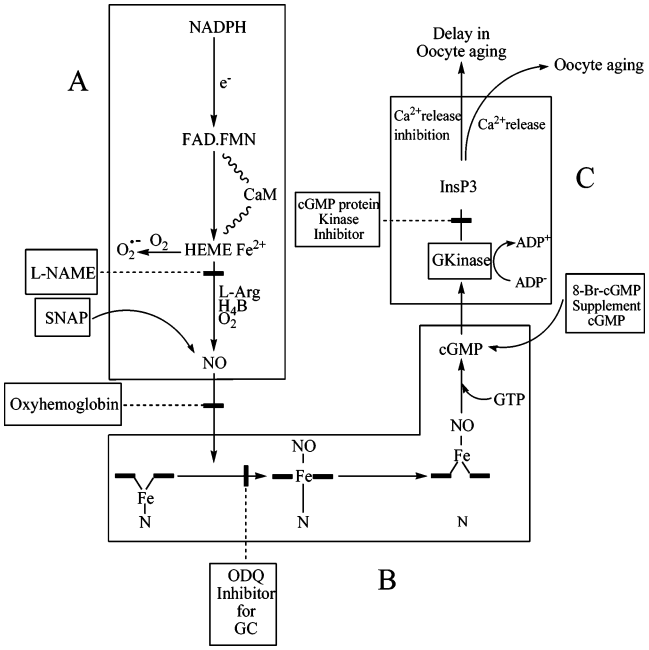

FIGURE 12: Model showing the role of NO and the involvement of the cGMP pathway in oocyte aging. Panel A illustrates the NOS catalytic cycle. In this cycle, the electron provided by NADPH first transfers to the NOS flavins and transfers them immediately to the NOS heme iron only when CaM binds. The NOS heme iron reduction enables the iron to bind and activate molecular oxygen and catalyze NO synthesis from L-Arg and H_4B. In the absence of L-Arg and/or cofactor H_4B, the reduction of NOS heme iron simply leads to $O_2^{\bullet -}$ generation. Panel B illustrates the GC catalytic cycle. In this cycle, the GC-Fe(II) ferrous binds to NO and forms a six-coordinate ferrous−nitrosyl complex. This process causes the trans axial ligand to break, thus forming a five-coordinate GC-Fe(II)−NO complex, which subsequently enables the enzyme to catalyze the conversion of GTP to cGMP. Panel C illustrates the G-kinase-induced Ca^{2+} release pathway. In this pathway, the enhancement of the cGMP level activates the cGMP-dependent protein kinase, which in turn catalyzes the phosphorylation of the InsP3 receptor leading to Ca^{2+} inhibition. Ca^{2+} release inhibition leads to a delay in oocyte aging, whereas Ca^{2+} release leads to oocyte aging. Exposing young and relatively old oocytes to L-NAME, oxyhemoglobin, ODQ, and a cGMP-dependent protein kinase inhibitor all enhanced oocyte aging phenomena. In parallel, supplementation with SNAP and 8-Br-cGMP delay oocyte aging.

Preventing oocyte aging is a useful approach to enhance the fertilizability of the oocytes and the developmental potential of the ensuing embryos, both in vivo and in vitro. Exploration of the NO-signaling mechanism related to oocyte physiology and aging as well as diabetes offers an option to correct this anomaly to improve the embryo outcome. Such an approach could be of value to enhance fertility in women in their middle 30s and beyond because chronological aging may also be associated with enhanced postovulatory aging (*14*, *69*, *70*). A correction of NO insufficiency in addition to tight glycemic control prior to pregnancy could reduce the occurrence of embryonic/fetal abnormalities and could, thereby, improve the pregnancy outcomes in diabetes mellitus.

In summary, the current study not only confirms our prior findings of the role of NO in delaying oocyte aging but also extends these observations to suggest the involvement of the cGMP pathway in this process. Furthermore, NO insufficiency could be a likely mechanism leading to enhanced oocyte aging that might occur under certain pathological conditions such as DM. Finally, the manipulation of NO within the oocyte and its microenvironment holds promise for enhancing/regulating fertility in vivo and in vitro as well as for the future development of new contraceptive technology.

REFERENCES

1. Lucas, M. J., Leveno, K. J., Williams, M. L., Raskin, P., and Whalley, P. J. (1989) Early pregnancy glycosylated hemoglobin, severity of diabetes, and fetal malformations, *Am. J. Obstet. Gynecol. 161*, 426−431.
2. Mills, J. L., Knopp, R. H., Simpson, J. L., Jovanovic-Peterson, L., Metzger, B. E., Holmes, L. B., Aarons, J. H., Brown, Z., Reed, G. F., Bieber, F. R., et al. (1988) Lack of relation of increased malformation rates in infants of diabetic mothers to glycemic control during organogenesis, *N. Engl. J. Med. 318*, 671−676.
3. Miller, E., Hare, J. W., Cloherty, J. P., Dunn, P. J., Gleason, R. E., Soeldner, J. S., and Kitzmiller, J. L. (1981) Elevated maternal hemoglobin A1c in early pregnancy and major congenital anomalies in infants of diabetic mothers, *N. Engl. J. Med. 304*, 1331−1334.
4. Greene, M. F. (1993) Prevention and diagnosis of congenital anomalies in diabetic pregnancies, *Clin. Perinatol. 20*, 533−547.
5. Diamond, M. P., Moley, K. H., Pellicer, A., Vaughn, W. K., and DeCherney, A. H. (1989) Effects of streptozotocin- and alloxan-induced diabetes mellitus on mouse follicular and early embryo development, *J. Reprod. Fertil. 86*, 1−10.
6. Colton, S. A., Humpherson, P. G., Leese, H. J., and Downs, S. M. (2003) Physiological changes in oocyte-cumulus cell complexes from diabetic mice that potentially influence meiotic regulation, *Biol. Reprod. 69*, 761−770.
7. Moley, K. H., Vaughn, W. K., DeCherney, A. H., and Diamond, M. P. (1991) Effect of diabetes mellitus on mouse pre-implantation embryo development, *J. Reprod. Fertil. 93*, 325−332.
8. Moley, K. H., Vaughn, W. K., and Diamond, M. P. (1994) Manifestations of diabetes mellitus on mouse preimplantation development: effect of elevated concentration of metabolic intermediates, *Hum. Reprod. 9*, 113−121.
9. Wilcox, A. J., Weinberg, C. R., and Baird, D. D. (1998) Post-ovulatory ageing of the human oocyte and embryo failure, *Hum. Reprod. 13*, 394−397.
10. Gray, R. H., Simpson, J. L., Kambic, R. T., Queenan, J. T., Mena, P., Perez, A., and Barbato, M. (1995) Timing of conception and the risk of spontaneous abortion among pregnancies occurring during the use of natural family planning, *Am. J. Obstet. Gynecol. 172*, 1567−1572.
11. Mailhes, J. B., Young, D., and London, S. N. (1998) Postovulatory aging of mouse oocytes in vivo and premature centromere separation and aneuploidy, *Biol. Reprod. 58*, 1206−1210.
12. Goud, P., Goud, A., Van Oostveldt, P., Van der Elst, J., and Dhont, M. (1999) Fertilization abnormalities and pronucleus size asynchrony after intracytoplasmic sperm injection are related to oocyte postmaturity, *Fertil. Steril. 72*, 245−252.
13. Goud, P. T., Goud, A. P., Laverge, H., De Sutter, P., and Dhont, M. (1999) Effect of post-ovulatory age and calcium in the injection medium on the male pronucleus formation and metaphase entry following injection of human spermatozoa into golden hamster oocytes, *Mol. Hum. Reprod. 5*, 227−233.
14. Eichenlaub-Ritter, U., and Boll, I. (1989) Nocodazole sensitivity, age-related aneuploidy, and alterations in the cell cycle during maturation of mouse oocytes, *Cytogenet. Cell Genet. 52*, 170−176.
15. Xu, Z., Abbott, A., Kopf, G. S., Schultz, R. M., and Ducibella, T. (1997) Spontaneous activation of ovulated mouse eggs: time dependent effects on M-phase exit, cortical granule exocytosis, maternal messenger ribonucleic acid recruitment, and inositol 1, 4, 5-trisphosphate sensitivity, *Biol. Reprod. 57*, 743−750.
16. Kikuchi, K., Naito, K., Noguchi, J., Shimada, A., Kaneko, H., Yamashita, M., Aoki, F., Tojo, H., and Toyoda, Y. (2000) Parthenogenesis and cytoskeletal organization in ageing mouse eggs, *Biol. Reprod. 63*, 715−722.
17. Webb, M., Howlett, S. K., and Maro, B. (1986) Parthenogenesis and cytoskeletal organization in aging mouse eggs, *J. Embryol. Exp. Morphol. 95*, 131−145.
18. Zernicka-Goetz, M., Kubiak, J. Z., Antony, C., and Maro, B. (1983) Cytoskeletal organization of rat oocytes during metaphase II arrest

and following abortive activation: a study by confocal laser scanning microscopy, *Mol. Reprod. Dev. 35*, 165−175.
19. Goud, A. P., Goud, P. T., Van Oostveldt, P., Diamond, M. P., and Dhont, M. (2004) Dynamic changes in microtubular cytoskeleton of human postmature oocytes revert after ooplasm transfer, *Fertil. Steril. 81*, 323−331.
20. Kikuchi, K., Naito, K., Noguchi, J., Shimada, A., Kaneko, H., Yamashita, M., Tojo, H., and Toyoda, Y. (1999) Inactivation of p34cdc2 kinase by the accumulation of its phosphorylated forms in porcine oocytes matured and aged in vitro, *Zygote 7*, 173−179.
21. Austin, C. R. (1956) Cortical granules in hamster eggs, *Exp. Cell Res. 10*, 533−540.
22. Braden, A. W., and Austin, C. R. (1954) The fertile life of mouse and rat eggs, *Science 120*, 610−611.
23. Yanagimachi, R., and Chang, M. C. (1961) Fertilizable life of golden hamster ova and their morphological changes at the time of losing fertilizability, *J. Exp. Zool. 148*, 185−203.
24. Szollosi, D. (1971) Morphological changes in mouse eggs due to aging in the fallopian tube, *Am. J. Anat. 130*, 209−225.
25. Longo, F. J. (1974) An ultrastructural analysis of spontaneous activation of hamster eggs aged in vivo, *Anat. Rec. 179*, 27−55.
26. O'Neill, G. T., and Kaufman, M. H. (1988) Influence of postovulatory aging on chromosome segregation during the second meiotic division in mouse oocytes: a parthenogenetic analysis, *J. Exp. Zool. 248*, 125−131.
27. Wautier, M. P., Chappey, O., Corda, S., Stern, D. M., Schmidt, A. M., and Wautier, J. L. (2001) Activation of NADPH oxidase by AGE links oxidant stress to altered gene expression via RAGE, *Am. J. Physiol.: Endocrinol. Metab. 280*, E685−694.
28. Inoguchi, T., Li, P., Umeda, F., Yu, H. Y., Kakimoto, M., Imamura, M., Aoki, T., Etoh, T., Hashimoto, T., Naruse, M., Sano, H., Utsumi, H., and Nawata, H. (2000) High glucose level and free fatty acid stimulate reactive oxygen species production through protein kinase C-dependent activation of NAD(P)H oxidase in cultured vascular cells, *Diabetes 49*, 1939−1945.
29. Brownlee, M. (2001) Biochemistry and molecular cell biology of diabetic complications, *Nature 414*, 813−820.
30. Nishikawa, T., Edelstein, D., Du, X. L., Yamagishi, S., Matsumura, T., Kaneda, Y., Yorek, M. A., Beebe, D., Oates, P. J., Hammes, H. P., Giardino, I., Brownlee, M. (2000) Normalizing mitochondrial superoxide production blocks three pathways of hyperglycaemic damage, *Nature 404*, 787−790.
31. Du, X. L., Edelstein, D., Dimmeler, S., Ju, Q., Sui, C., and Brownlee, M. (2001) Hyperglycemia inhibits endothelial nitric oxide synthase activity by posttranslational modification at the Akt site, *J. Clin. Invest. 108*, 1341−1348.
32. Khorram, O. (2002) Nitric oxide and its role in blastocyst implantation, *Rev. Endocr. Metab. Disord. 3*, 145−149.
33. Nishimi, A., Matsukawa, T., Hoshino, K., Ikeda, S., Kira, Y., Sato, E. F., Inoue, M., and Yamada, M. (2001) Localization of nitric oxide synthase activity in unfertilized oocytes and fertilized embryos during preimplantation development in mice, *Reproduction 122*, 957−963.
34. Griffith, O. W., and Stuehr, D. J. (1995) Nitric oxide synthases: properties and catalytic mechanism, *Annu. Rev. Physiol. 57*, 707−736.
35. Galijasevic, S., Saed, G. M., Diamond, M. P., and Abu-Soud, H. M. (2003) Myeloperoxidase up-regulates the catalytic activity of inducible nitric oxide synthase by preventing nitric oxide feedback inhibition, *Proc. Natl. Acad. Sci. U.S.A. 100*, 14766−14771.
36. Ignarro, L. J. (1990) Haem-dependent activation of guanylate cyclase and cyclic GMP formation by endogenous nitric oxide: a unique transduction mechanism for transcellular signaling, *Pharmacol. Toxicol. 67*, 1−7.
37. Stone, J. R., and Marletta, M. A. (1996) Spectral and kinetic studies on the activation of soluble guanylate cyclase by nitric oxide, *Biochemistry 35*, 1093−1099.
38. Kelm, M., Feelisch, M., Spahr, R., Piper, H. M., Noack, E., and Schrader, J. (1988) Quantitative and kinetic characterization of nitric oxide and EDRF released from cultured endothelial cells, *Biochem. Biophys. Res. Commun. 154*, 236−244.
39. Moncada, S., Palmer, R. M., and Higgs, E. A. (1991) Nitric oxide: Physiology, pathophysiology, and pharmacology, *Pharmacol. Ther. 56*, 191−231.
40. Goud, P. T., Goud, A. P., Leybaert, L., Van Oostveldt, P., Mikoshiba, K., Diamond, M. P., and Dhont, M. (2002) Inositol 1, 4, 5-trisphosphate receptor function in human oocytes: calcium responses and oocyte activation-related phenomena induced by photolytic release of InsP(3) are blocked by a specific antibody to the type I receptor, *Mol. Hum. Reprod. 8*, 912−918.
41. Goud, A. P., Goud, P. T., Diamond, M. P., and Abu-Soud, H. M. (2005) Nitric oxide delays oocyte aging, *Biochemistry 44*, 11361−11368.
42. Goud, A. P., Goud, P. T., Van Oostveldt, P., Diamond, M. P., and Hughes, M. R. (2005) Microtubule turnover in ooplasm biopsy reflects aging related phenomena in the parent oocyte, *Reprod. BioMed. Online 11*, 43−52.
43. Chen, H. W., Jiang, W. S., Tzeng, C. R. (2001) Nitric oxide as a regulator in preimplantation embryo development and apoptosis, *Fertil. Steril. 75*, 1163−1171.
44. Glass, D. B., and Smith, S. B. (1983) Phosphorylation by cyclic GMP-dependent protein kinase of a synthetic peptide corresponding to the autophosphorylation site in the enzyme, *J. Biol. Chem. 258*, 14797−14803.
45. Aoki, F., Worrad, D. M., and Schultz, R. M. (1997) Regulation of transcriptional activity during the first and second cell cycles in the preimplantation mouse embryo, *Dev. Biol. 181*, 296−307.
46. Cai, S., Khoo, J., Mussa, S., Alp, N. J., and Channon, K. M. (2005) Endothelial nitric oxide synthase dysfunction in diabetic mice: importance of tetrahydrobiopterin in eNOS dimerisation, *Diabetologia 48*, 1933−1940.
47. Bitar, M. S., Wahid, S., Mustafa, S., Al-Saleh, E., Dhaunsi, G. S., and Al-Mulla, F. (2005) Nitric oxide dynamics and endothelial dysfunction in type II model of genetic diabetes, *Eur. J. Pharmacol. 511*, 53−64.
48. Srinivasan, S., Hatley, M. E., Bolick, D. T., Palmer, L. A., Edelstein, D., Brownlee, M., and Hedrick, C. C. (2004) Hyperglycaemia-induced superoxide production decreases eNOS expression via AP-1 activation in aortic endothelial cells, *Diabetologia 47*, 1727−1734.
49. De Vriese, A. S., Verbeuren, T. J., Van de Voorde, J., Lameire, N. H., and Vanhoutte, P. M. (2000) Endothelial dysfunction in diabetes, *Br. J. Pharmacol. 130*, 963−974.
50. Abu-Soud, H. M., and Stuehr, D. J. (1993) Nitric oxide synthases reveal a role for calmodulin in controlling electron transfer, *Proc. Natl. Acad. Sci. U.S.A. 90*, 10769−10772.
51. Abu-Soud, H. M., Yoho, L. L., and Stuehr, D. J. (1994) Calmodulin controls neuronal nitric-oxide synthase by a dual mechanism. Activation of intra- and interdomain electron transfer, *J. Biol. Chem. 269*, 32047−32050.
52. Abu-Soud, H. M., Ichimori, K., Presta, A., and Stuehr, D. J. (2000) Electron transfer, oxygen binding, and nitric oxide feedback inhibition in endothelial nitric-oxide synthase, *J. Biol. Chem. 275*, 17349−17357.
53. Rosen, G. M., Tsai, P., Weaver, J., Porasuphatana, S., Roman, L. J., Starkov, A. A., Fiskum, G., and Pou, S. (2002) The role of tetrahydrobiopterin in the regulation of neuronal nitric-oxide synthase-generated superoxide, *J. Biol. Chem. 277*, 40275−40280.
54. Garbers, D. L., and Lowe, D. G. (1994) Guanylyl cyclase receptors, *J. Biol. Chem. 69*, 30741−30744.
55. Waldman, S. A., and Murad, F. (1987) Cyclic GMP synthesis and function, *Pharmacol. Rev. 39*, 163−196.
56. Denninger, J. W., and Marletta, M. A. (1990) Guanylate cyclase and the NO/cGMP signaling pathway, *Biochim. Biophys. Acta 1411*, 334−350.
57. Tomita, T., Ogura, T., Tsuyama, S., Imai, Y., and Kitagawa, T. (1997) Effects of GTP on bound nitric oxide of soluble guanylate cyclase probed by resonance Raman spectroscopy, *Biochemistry 36*, 10155−10160.
58. Armstrong, D. T. (2001) Effects of maternal age on oocyte developmental competence, *Teriogenology 55*, 1303−22.
59. Hassold, T., and Chiu, D. (1985) Maternal age-specific rates of numerical chromosome abnormalities with special reference to trisomy, *Hum. Genet. 70*, 11−17.
60. Walter, U., Eigenthaler, M., Geiger, J., and Reinhard, M. (1993) Role of cyclic nucleotide-dependent protein kinases and their common substrate VASP in the regulation of human platelets, *Adv. Exp. Med. Biol. 344*, 237−249.
61. Lincoln, T. M., Komalavilas, P., Boerth, N. J., MacMillan-Crow, L. A., and Cornwell, T. L. (1955) cGMP signaling through cAMP-cGMP-dependent protein kinases, *Adv. Pharmacol. 34*, 305−322.
62. Butt, E., Nolte, C., Schulz, S., Beltman, J., Beavo, J. A., Jastroff, B., and Walter, U. (1992) Analysis of the fuctional role of c GMP-dependent protein kinase in intact human platelets using a specific

activator 8-para-cholrophenylthio-cGMP, *Biochem. Pharmacol. 43*, 2591−2600.
63. Tertyshnikova, S., Yan, X., Fein, A. (1998) cGMP inhibits IP3-induced Ca^{2+} release in intact rat megakaryocytes via cGMP- and cAMP-dependent protein kinases, *J. Physiol. 512*, 89−96.
64. Deana, R., Ruzzene, M., Doni, M. G., Zoccarato, F., and Alexandre, A. (1989) Interaction of nitric oxide and cGMP with signal transduction in activated platelets, *Biochim. Biophys. Acta 1014*, 203−206.
65. Nguyen, B., Saiton, M., and Ware, J. A. (1991) Mechanism of cyclic GMP inhibition of inositol phosphate formation in rat aorta segments and cultured bovine aortic smooth muscle cells, *Am. J. Physiol. 261*, H1043−H1051.
66. Hirata, M., Kohse, K. P., Chang, C. H., Ikebe, T., and Murad, F. (1990) Mechanism of cyclic GMP inhibition of inositol phosphate formation in rat aorta segments and cultured bovine aortic smooth muscle cells, *J. Biol. Chem. 265*, 1268−1273.
67. Kuo, R. C., Baxter, G. T., Thompson, S. H., Stricker, S. A., Patton, C., Bonaventura, J., and Epel, D. (2000) NO is necessary and sufficient for egg activation at fertilization, *Nature 406*, 633−636.
68. Takahashi, T., Takahashi, E., Igarashi, H., Tezuka, N., and Kurachi, H. (2003) Impact of oxidative stress in aged mouse oocytes on calcium oscillations at fertilization, *Mol. Reprod. Dev. 66*, 143−152.
69. Keefe, D. L. (1997) Aging and infertility in women, *Med. Health R.I. 80*, 403−405.
70. Eichenlaub-Ritter, U. (1998) Genetics of oocyte aging, *Maturitas 30*, 143−169.

BI060910E